Expression of BSP-GFPtpz Transgene during Osteogenesis and Reparative Dentinogenesis

Vijaykumar, A.; Dyrkacz, P.; Vidovic-Zdrilic, Ivana; Maye, P.; Mina, M.

Journal of Dental Research
2020, Vol. 99(1) 89–97

DOI: 10.1177/0022034519885089
journals.sagepub.com/home/jdr

Expression of BSP-GFPtpz Transgene during Osteogenesis and Reparative Dentinogenesis

A. Vijaykumar[1], P. Dyrkacz[1], I. Vidovic-Zdrilic[1], P. Maye[2], and M. Mina[1]

Abstract

Bone sialoprotein (BSP) is a member of the SIBLING family with essential roles in skeletogenesis. In the developing teeth, although the expression and function of BSP in the formation of acellular cementum and periodontal attachment are well documented, there are uncertainties regarding the expression and function of BSP by odontoblasts and dentin. Reporter mice are valuable animal models for biological research, providing a gene expression readout that can contribute to cellular characterization within the context of a developmental process. In the present study, we examined the expression of a BSP-GFPtpz reporter mouse line during odontoblast differentiation, reparative dentinogenesis, and bone. In the developing teeth, BSP-GFPtpz was expressed at high levels in cementoblasts but not in odontoblasts or dentin. In bones, the transgene was highly expressed in osteoblasts at an early stage of differentiation. Interestingly, despite its lack of expression in odontoblasts and dental pulp during tooth development, the BSP-GFPtpz transgene was detected during in vitro mineralization of primary pulp cultures and during reparative dentinogenesis following pulp exposures. Importantly, under these experimental contexts, the expression of BSP-GFPtpz was still exclusive to DSPP-Cerulean, an odontoblast-specific reporter gene. This suggests that the combinatorial use of BSP-GFPtpz and DSPP-Cerulean can be a valuable experimental tool to distinguish osteogenic from dentinogenic cells, thereby providing an avenue to investigate mechanisms that distinctly regulate the lineage progression of progenitors into odontoblasts versus osteoblasts.

Keywords: odontoblasts, bone, bone sialoprotein, reparative dentin, fluorescent protein reporters, osteoblasts

Introduction

Bone and dentin are distinct mineralized tissues that display morphologic and functional differences. Despite these differences, they share similarities in their mineralization process. During this process, osteoblasts and odontoblasts first secrete unmineralized matrices termed *osteoid* and *predentin*, respectively. The organic component of osteoid and predentin consists of extracellular matrix composed of primarily type I collagen and several noncollagenous proteins that play essential roles in the mineralization of collagen fibers during the conversion of osteoid and predentin to bone and dentin, respectively.

One gene family contributing to the noncollagenous proteins of bone and dentin is the SIBLING family (small integrin-binding ligand, N-linked glycoprotein; Bellahcene et al. 2008; Staines et al. 2012; Bouleftour et al. 2016). SIBLING proteins comprise a structurally and phylogenetically homogenous group of 5 glycophosphoproteins, named osteopontin, bone sialoprotein (BSP), dentin matrix protein 1 (DMP1), dentin sialophosphoprotein (DSPP), and matrix extracellular phosphoglycoprotein.

SIBLING proteins share many common features (Bellahcene et al. 2008; Staines et al. 2012; Bouleftour et al. 2016), including their common chromosomal localization as a genetically linked cluster covering a 375-kb region on human chromosome 4q21 and mouse chromosome 5q. Additionally, different genes within this family share a similar exon structure and the RGD motifs enabling them to propagate biological signals by initiating integrin-mediated signaling (Bellahcene et al. 2008; Staines et al. 2012; Bouleftour et al. 2016).

Despite these similarities, genes within this family display differences in their tissue expression and functions. The specific functions of SIBLING family members in bone and dentin have been revealed through various genetic mouse models and linkage to human diseases (Bellahcene et al. 2008; Staines et al. 2012; Bouleftour et al. 2016).

BSP (integrin binding sialoprotein) is a 70- to 80-kDa extracellular matrix protein with essential roles in skeletogenesis (Staines et al. 2012). Unlike other SIBLING proteins, BSP is

[1]Department of Craniofacial Sciences, School of Dental Medicine, University of Connecticut, Farmington, CT, USA
[2]Department of Reconstructive Sciences, School of Dental Medicine, University of Connecticut, Farmington, CT, USA

A supplemental appendix to this article is available online.

Corresponding Author:
M. Mina, Division of Pediatric Dentistry, Department of Craniofacial Sciences, School of Dental Medicine, University of Connecticut Health, 260 Farmington Ave, Farmington, CT 06030, USA.
Email: mina@uchc.edu

exclusively found in mineralized tissues with essential roles in the initial formation of hydroxyapatite (Staines et al. 2012; Bouleftour et al. 2016). Abnormalities in the Bsp-null mouse revealed the essential roles of BSP in bone growth and mineralization (Staines et al. 2012; Bouleftour et al. 2016).

In the developing teeth, although the expression and function of BSP in the formation of acellular cementum and periodontal attachment are well documented (Bosshardt et al. 1998; Foster et al. 2013; Foster et al. 2015), there are controversial reports regarding the expression and function of BSP by odontoblasts during physiologic dentinogenesis. Several studies have reported the expression of BSP in odontoblasts and physiologic dentin (Butler and Ritchie 1995; Ganss et al. 1999; Fisher and Fedarko 2003; Chen et al. 2008), whereas others reported BSP expression only in tertiary dentin (James et al. 2004; Yang et al. 2010; Vidovic et al. 2017). Furthermore, in dentin, a relatively low level (Fujisawa et al. 1993; Ganss et al. 1999; Bouleftour et al. 2016) to levels similar to bone (Qin et al. 2001; Bouleftour et al. 2016) has been reported.

By allowing the visualization of gene expression under various in vivo and in vitro conditions, fluorescent protein reporter mice have provided valuable animal models for biological studies. Given the uncertainty regarding the expression of BSP by odontoblasts and physiologic dentin and the essential roles of BSP in mineralization, in the present study we examined the expression of BSP and BSP-GFPtpz transgene in the developing teeth and bones and in reparative dentinogenesis with Bsp-GFPtpz transgenic mice (Maye et al. 2009).

Materials and Methods

Animal Models and Analyses of Expression of Transgenes In Vivo

BSP-GFPtpz and DSPP-Cerulean/DMP1-Cherry transgenic mice have been previously described (Maye et al. 2009; Vijaykumar et al. 2019). BSP-GFPtpz/DSPP-Cerulean/DMP1-Cherry mice were generated by crossing BSP-GFPtpz with DSPP-Cerulean/DMP1-Cherry mice. Animal protocols were approved by Institutional Animal Care. All mice were maintained in the CD1 background.

The expression of transgenes was characterized in serial sections. Mandibular arches, long bones, and calvarias were fixed overnight in 4% paraformaldehyde, decalcified, and processed for cryosectioning (Dyment et al. 2016). Sections were mounted with 30% glycerol and examined with a Zeiss Axio Observer Z1 inverted microscope with filter cubes optimized for the detection of different fluorescent proteins. The full-size images were obtained by scanning at high power, followed by stitching the scans into a composite. Exposure times were adjusted for optimum imaging and kept consistent throughout the various time points.

Cell Cultures, Digital Imaging, and Epifluorescence Analysis. Primary cultures from dental pulp were prepared from 5- to 7-d-old hemizygous BSP-GFPtpz, BSP-GFPtpz/DSPP-Cerulean/DMP1-Cherry, and nontransgenic mice (Vijaykumar et al. 2019). Mineralization in live cultures was examined by xylenol orange staining (20 μM overnight; Balic and Mina 2005). Live cultured cells were imaged for detection of various fluorescent proteins at different time points.

Immunocytochemistry. Mandibular arches, long bones, calvarias, and adult maxillary arches with pulp exposures were processed for immunocytochemistry with anti-BSP primary antibody (1:100, bs-2668R; Bioss USA) and goat anti-rabbit AF488 (1:400, A11001; Invitrogen) or donkey anti-rabbit Cy3 secondary antibodies (1:200; Jackson ImmunoResearch). Sections were also processed for staining with 1:1,000 dilution of anti-GFP Alexa Fluor 488–conjugated antibody (Molecular Probes, Invitrogen).

RNAscope In Situ Hybridization. In situ hybridization was conducted in frozen sections with the RNAscope 2.5 HD Reagent Kit-BROWN (Advanced Cell Diagnostics) for *Bsp* as described previously (Vidovic et al. 2017).

Flow Cytometric Analysis. Single-cell suspensions from pulp cultures were processed for fluorescence-activated cell sorting (FACS) analysis at different time points with gating strategies shown in Appendix Figures 1 and 3. Pulp cells from nontransgenic littermates served as negative control in all experiments. Percentages of GFP^+ and GFP^- cells were determined with BD FACSDiva 6.2 software.

RNA Extraction and Analyses. Total RNA was prepared with TRIzol Reagent according to the manufacturer's instructions. After DNase treatment, RNA samples were processed for cDNA synthesis and reverse transcription polymerase chain reaction analysis with specific primers (Appendix Fig. 2).

Experimental Pulp Exposure/Injury. Four-week-old transgenic mice were anesthetized and prepared for experimental pulp exposure on the maxillary first molars (Vidovic et al. 2017; Vidovic-Zdrilic et al. 2018). Animals were sacrificed at 0 d, 2 wk, and 4 wk after injury and then fixed and processed for cryosectioning and analyses. The adjacent sections were processed for staining with hematoxylin and eosin and anti-BSP antibody.

Statistical Analysis. Data analysis was performed by Graph Pad Prism 6 software with unpaired 2-tailed Student's *t* test. Values in all experiments represented the mean ± SEM of at least 3 to 5 independent experiments, and a P value ≤ 0.05 was considered statistically significant.

Results

Expression of BSP-GFPtpz in the Developing Teeth and Alveolar Bones

We examined the expression of BSP-GFPtpz transgene in mandibular arches during embryonic development (E15 to E20) and postnatal growth (P1, P6, P30). While BSP-GFPtpz

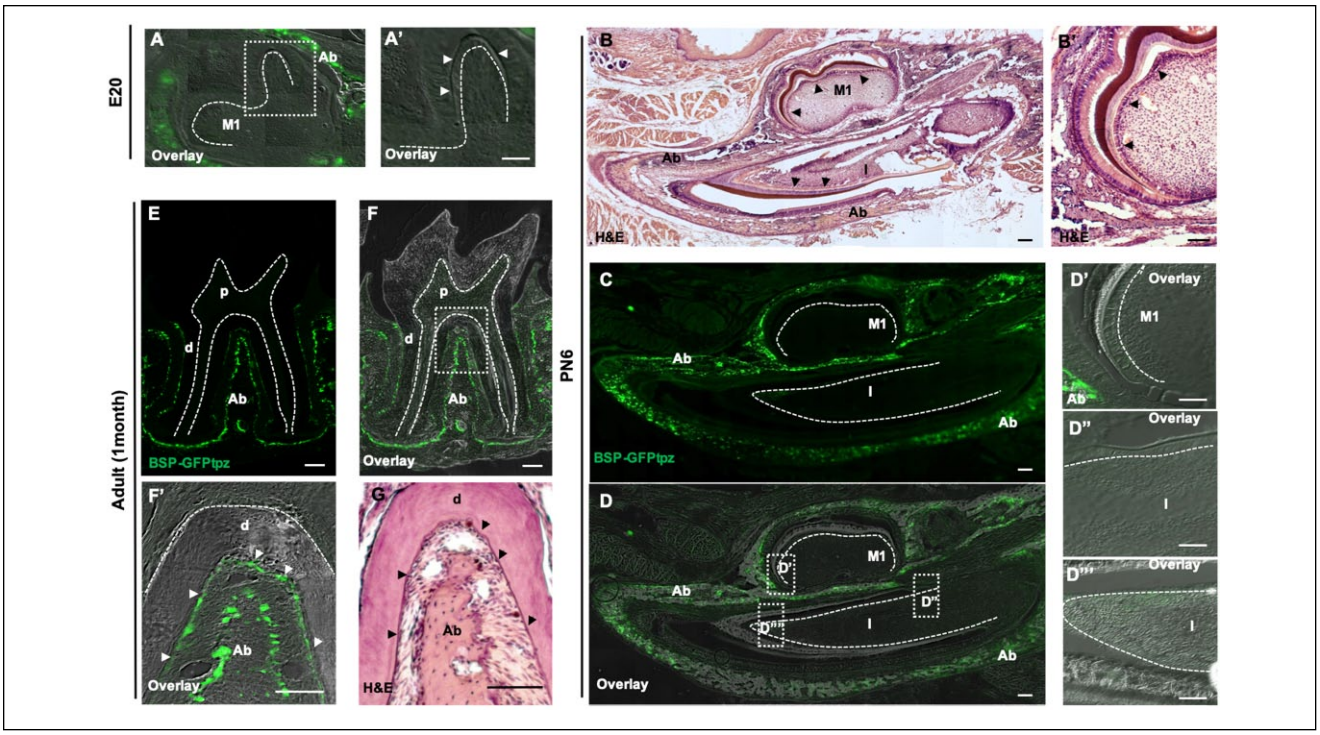

Figure 1. Expression of BSP-GFPtpz in the developing teeth and alveolar bone of mice. (**A**, **A**′) A cross section of the mandibular first molar at E20. Note the expression of BSP-GFPtpz in the alveolar bone surrounding the unerupted molar and the lack of expression in the odontoblast layer (arrowheads in A′). (A′) A higher-magnification image of the boxed area in panel A. (**B**, **B**′) An H&E-stained sagittal section through the lower jaw at P6. (B′) A higher-magnification image of the boxed area in panel B. Odontoblast layer in the first molar and incisor is indicated by arrowheads. (**C–D**‴) Epifluorescent images of adjacent section to panel B. (D′–D‴) Images at higher magnification of the boxed areas in panel D. Note the expression of BSP-GFPtpz in the alveolar bone surrounding the unerupted molar and incisor and the lack of transgene expression in the odontoblasts in the first molar and incisor. (**E–G**) Epifluorescent images of a section through a mandibular molar at 1 mo of age. (F′) A higher-magnification image of the boxed area in panel F. (G) An H&E-stained image of an adjacent section. BSP-GFPtpz is expressed in cementoblasts lining the cementum (arrowheads) and osteoblasts in the alveolar bone. In all images, the pulp chambers are denoted by dashed lines. Ab, alveolar bone; d, dentin; H&E, hematoxylin and eosin; I, incisor; M1, first molar; p, dental pulp. Scale bar in all images: 100 µm.

was highly expressed in the alveolar bone, transgene expression was not detected in the developing tooth at the bud-to-bell stages of development (Fig. 1A, A′ and data not shown). At the secretory stage of crown formation (P1 to P6), BSP-GFPtpz transgene was not detected in the undifferentiated or differentiated odontoblasts surrounding dental pulp in the unerupted molars (Fig. 1B–D‴ and data not shown). In the erupted molars (1 mo old), BSP-GFPtpz transgene was expressed in cementoblasts lining the root cementum but not in the odontoblasts lining coronal and radicular pulp chamber (Fig. 1E–G). In the developing incisors that display an apical-to-incisal gradient of odontoblast differentiation, BSP-GFPtpz expression was not detected in the entire odontoblast layer (Fig. 1B–D‴). BSP-GFPtpz expression was not detected in dental pulp.

To ensure that the lack of transgene detection in odontoblasts was not related to loss of signal during the histologic processing, we also examined transgene expression by immunostaining for GFP (Fig. 2A, a–d). Immunostaining with anti-GFP antibody also showed expression in the alveolar bones but not in odontoblasts (Fig. 2A, a–d). To determine whether the reporter gene accurately represented endogenous gene expression, we compared the expression of BSP-GFPtpz with the expression of endogenous BSP protein (Fig. 2A, e, f) and *Bsp* (Fig. 2A, g, h) by immunohistochemistry and RNAscope, respectively. These studies together also confirmed high levels of expression of BSP and *Bsp* in the osteoblasts and in bone matrix. BSP and *Bsp* were not detected in dentin and odontoblasts, respectively.

Expression of BSP-GFPtpz Transgene in Long Bones and Calvarias In Vivo

For the next step, we examined the expression of the transgene in the long bones (Fig. 2B) and calvarias at P1 and P6 (Fig. 2C). In the developing long bones, BSP-GFPtpz was expressed at high intensity in osteoblasts lining the trabecular bone surfaces (just below the growth plate) and cortical bone surfaces and within the secondary ossification centers (Fig. 2B). BSP-GFPtpz was also expressed at lower intensity in osteocytes, many of which were in close proximity to the bone surfaces but embedded within bone tissue.

In the calvarias (P1 and P6), BSP-GFPtpz transgene was expressed in osteoblasts lining the periosteum and in some of osteocytes embedded within the calvaria bone (Fig. 2C). The

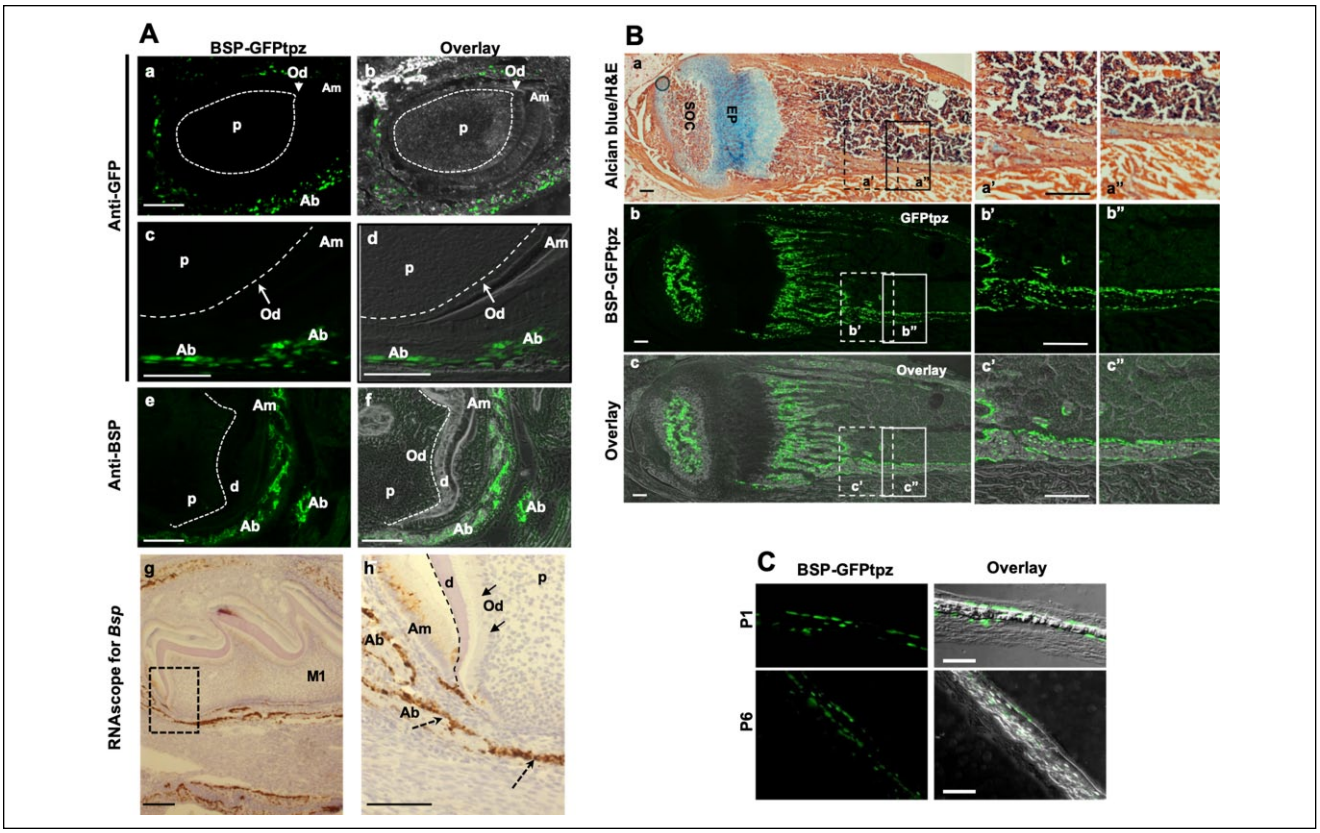

Figure 2. Expression of BSP-GFPtpz transgene in teeth, long bones, and calvarias. (**A**) Similarities in the expression of BSP-GFPtpz transgene, endogenous BSP, and *Bsp*. (a–f) Images of cross sections through an incisor (a, b) and a first molar (c–f) in the lower jaw at P6. Sections were stained with anti-GFP antibody (a–d) and anti-BSP antibody (e, f). Sections were permeabilized (0.3% TritonX-100 for 20 min), washed and incubated with PowerBlock reagent for 20 min at room temperature, incubated overnight at 4 °C with anti-GFP AF488-conjugated antibody (1:1,000; Molecular Probes, Invitrogen) or rabbit anti-BSP primary antibody (1:100, bs-2668R; Bioss USA), with the latter followed by goat anti-rabbit AF488 secondary antibody (1:400, A11001; Invitrogen) for 1 h at room temperature. Note GFP staining in the osteoblasts in the alveolar bones but not in odontoblasts (arrows; a–d). Also note BSP staining in the alveolar bone matrix but not in dentin (e, f). (g, h) Images through a first molar in the lower jaw at P6. (h) A higher magnification of the boxed area in panel g. Section was processed for RNAscope in situ hybridization for *Bsp*, showing the expression of *Bsp* in osteoblasts of the alveolar bone (dashed arrow) but not in odontoblasts (solid arrows). In all images, the pulp chambers are denoted by dashed lines. Scale bar in all images in panel A: 100 µm. (**B**) Expression of BSP-GFPtpz transgene in long bone. (a–a″) Representative images of sections through a long bone at P6 from BSP-GFPtpz mice stained with alcian blue and H&E show the secondary ossification center (SOC) and epiphyseal plate (EP). (a′, a″) Higher magnifications of the dashed and solid boxed areas in panel a. (b, c) Epifluorescent images of an adjacent section to panel a show high levels of expression of BSP-GFPtpz in osteoblasts and osteocytes. (b′–c″) Higher magnification of boxed areas in panels b and c. Scale bars in panels a–c: 500 µm. Scale bars in panels a′–c″: 100 µm. (**C**) Expression of BSP-GFPtpz transgene in calvaria. Representative images of calvaria at P1 and P6 from BSP-GFPtpz mice show high levels of BSP-GFPtpz in osteoblasts in periosteum and some of the osteocytes. Scale bar in all images in panel C: 100 µm. Ab, alveolar bone; Am, ameloblasts; d, dentin; H&E, hematoxylin and eosin; M1, first molar; Od, odontoblasts; p, dental pulp.

patterns of expression of BSP-GFPtpz in calvaria and long bone are consistent with previously reported expression of BSP (Foster et al. 2015; Bouleftour et al. 2016) and BSP-GFPtpz (Maye et al. 2009; Strecker et al. 2013; Fu and Maye 2015).

Comparison of the Expression of BSP-GFPtpz and DMP1-Cherry Transgenes in Long Bones and Calvaria In Vivo

The expression of BSP-GFPtpz in osteoblasts and osteocytes is similar to the expression of DMP1 (Qin et al. 2007) and DMP1-Cherry transgene (Vijaykumar et al. 2019). Therefore, we decided to compare the expression of BSP-GFPtpz to DMP1-Cherry in long bones (Fig. 3A) and calvaria (Fig. 3B) with BSP-GFPtpz/DSPP-Cerulean/DMP1-Cherry mice. These experiments showed overlapping and nonoverlapping expression domains for BSP-GFPtpz and DMP1-Cherry in osteoblasts and osteocytes.

In the mature bones, BSP-GFPtpz was highly expressed in osteoblasts closer to the growth plate, and DMP1-Cherry was expressed in more osteoblasts at a further distance from the growth plate (Fig. 3A). There were few cells coexpressing both transgenes at the interface between BSP-GFPtpz^{+} and DMP1-Cherry^{+} domains (Fig. 3Aa″). In the cortical bone, DMP1-Cherry was highly expressed in all osteocytes, whereas BSP-GFPtpz was detected in only a small subpopulation of osteocytes often closer to bone surfaces (Fig. 3Aa′).

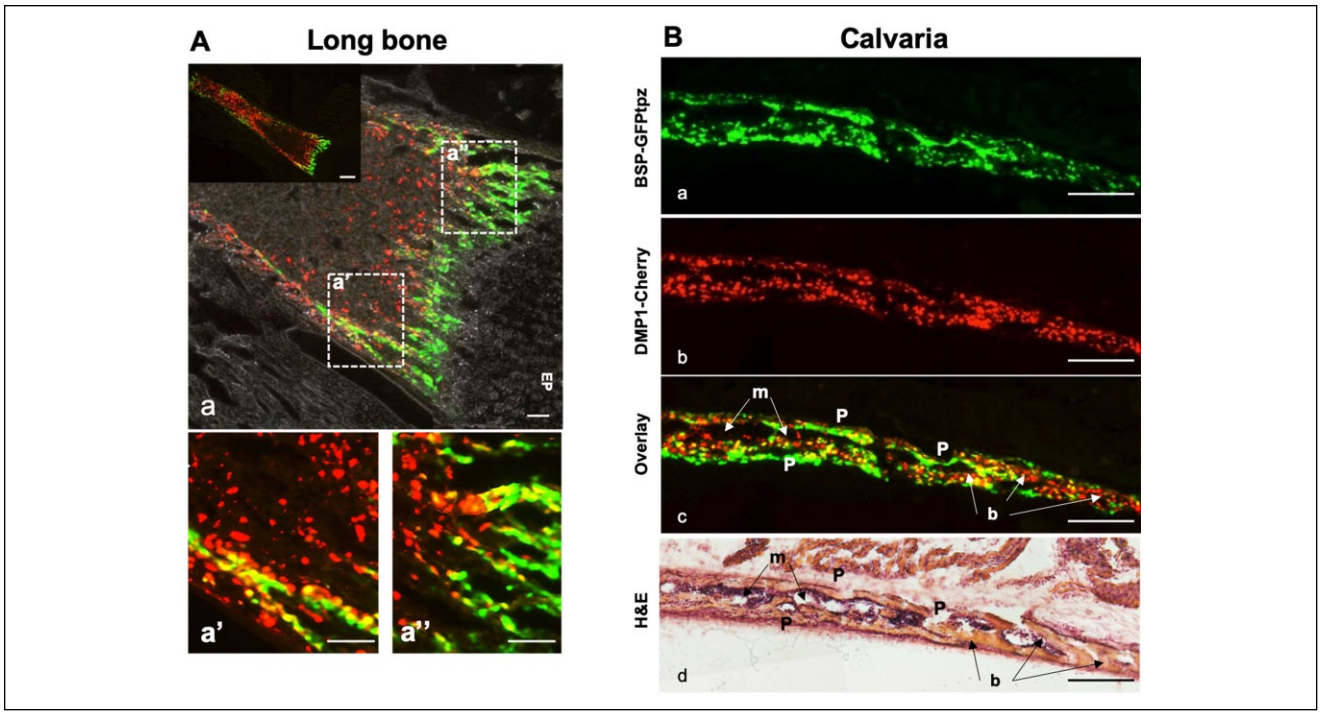

Figure 3. Expression of BSP-GFPtpz and DMP1-Cherry transgenes in the long bones and calvaria. (**A**) Representative images of a long bone at P6 from BSP-GFPtpz/DSPP-Cerulean/DMP1-Cherry mice show the overlapping and nonoverlapping domains of expression of BSP-GFPtpz and DMP1-Cherry in osteoblasts and osteocytes. (a) Inset shows the scan of a long bone. (a′, a″) Higher magnification of the boxed areas in panel a shows the overlapping expression in yellow. Note that BSP-GFPtpz is expressed at high levels in osteoblasts closer to the growth plate as compared with DMP1-Cherry^{+} cells. Also, note the higher-intensity expression of DMP1-Cherry in osteocytes as compared with BSP-GFPtpz. Scale bar inset: 500 µm. Scale bar in panels a–a″: 100 µm. (**B**) Representative images of a calvaria at P6 from BSP-GFPtpz/DSPP-Cerulean/DMP1-Cherry mice show the overlapping and nonoverlapping domains of expression of BSP-GFPtpz and DMP1-Cherry in osteoblasts and osteocytes. Representative epifluorescent images show the expression of BSP-GFPtpz (a), DMP1-Cherry^{+} (b), and overlay (c) of expression. (d) H&E-stained adjacent section. b, bone; EP, epiphyseal plate; H&E, hematoxylin and eosin; m, marrow cavity, p, periosteum. Scale bar: 500 µm.

In the calvaria, there were also very few cells coexpressing both transgenes. BSP-GFPtpz was highly expressed in osteoblasts lining the periosteum and the bone marrow cavities (Fig. 3B). However, DMP1-Cherry was highly expressed in osteocytes embedded in bone. As reported previously, DSPP-Cerulean expression was not detected in long bones and calvaria (data not shown and Vijaykumar et al. 2019). Together these observations indicated that BSP-GFPtpz is highly expressed by osteoblasts in early stages of maturation, whereas DMP1-Cherry is expressed in osteoblasts in late stages of maturation.

Evaluation of BSP-GFPtpz Transgene Expression in Primary Dental Pulp Cultures In Vitro

Previous studies have shown that the primary pulp cultures contained progenitors capable of giving rise to osteoblasts and odontoblasts (Zhao et al. 2007; Takamori et al. 2008; Balic and Mina 2011). Therefore, as the next step, we examined the temporal and spatial expression of the BSP-GFPtpz transgene during in vitro mineralization in primary pulp cultures by epifluorescence and FACS analysis (Fig. 4; Appendix Figs. 1, 3, 4).

FACS analysis showed that freshly isolated pulps did not contain BSP-GFPtpz^{+} cells (Appendix Fig. 1C). When placed in culture, a few cells expressing BSP-GFPtpz at low intensity appeared at day 4 (Appendix Fig. 1C). With the onset of mineralization at day 10, there was an approximately 3-fold increase in the percentage of BSP-GFPtpz^{+} cells, followed by marked increases in BSP-GFPtpz^{+} cells with further mineralization of cultures (Fig. 4A; Appendix Figs. 1, 2). BSP-GFPtpz expression was detected in multilayered areas containing mineralized matrices detected by xylenol orange staining (Fig. 4A, q–s).

Reverse transcription polymerase chain reaction showed that the expression of transgene during in vitro mineralization was well correlated with the expression of endogenous *Bsp.* Similar to *Bsp*, BSP-GFPtpz was expressed at very low levels at day 7 with marked increases at days 10 to 21 (Appendix Fig. 2B).

The expression of BSP-GFPtpz was also compared with the expression of DSPP-Cerulean and DMP1-Cherry during the in vitro mineralization of primary pulp cultures by epifluorescence and FACS analysis (Fig. 4B; Appendix Fig. 3). These studies showed nonoverlapping and exclusive expression of BSP-GFPtpz and DSPP-Cerulean transgenes (Fig. 4B; Appendix Fig. 3A–C), confirming the lack of BSP-GFPtpz expression in DSPP-Cerulean^{+} odontoblasts. However, there

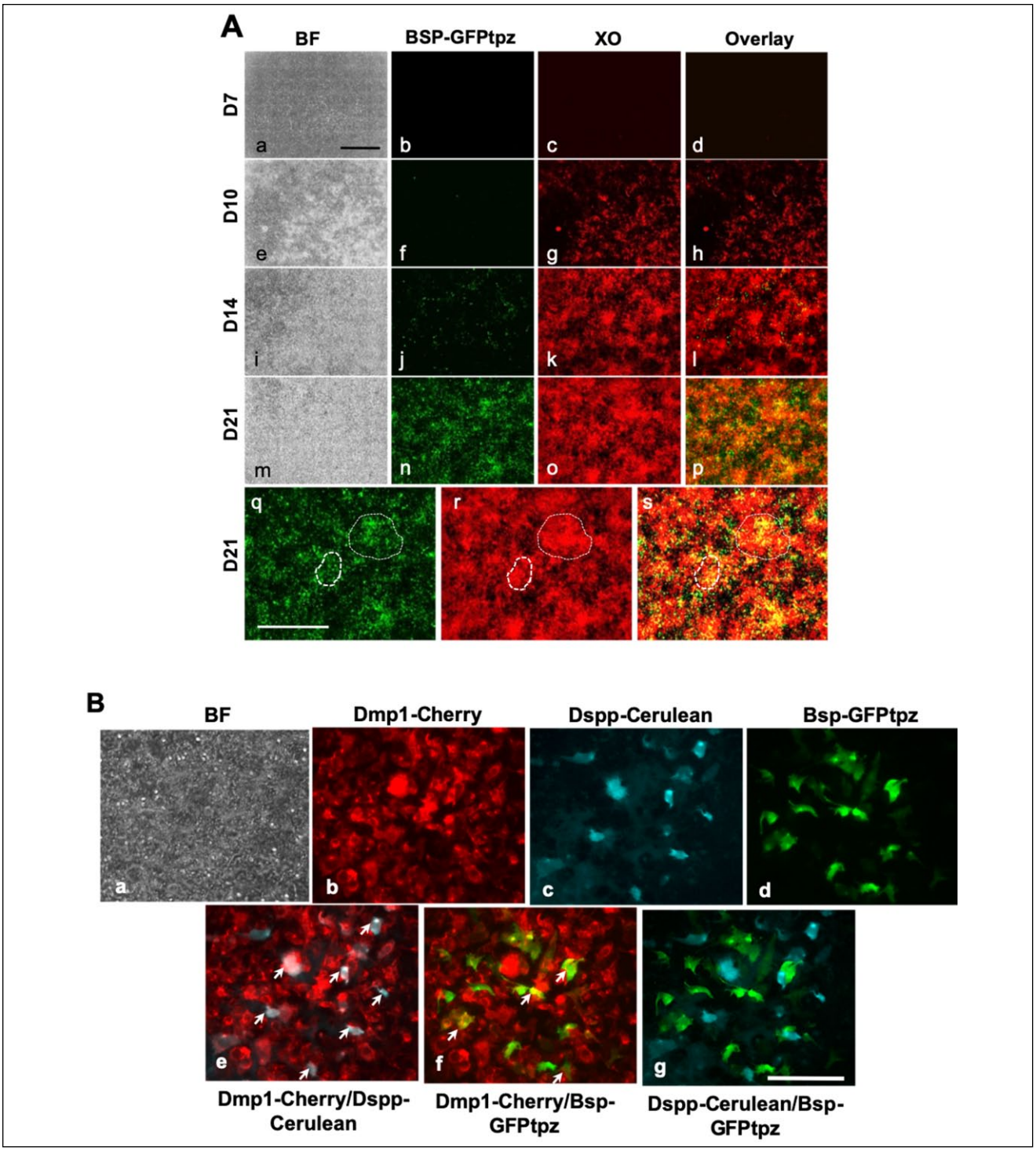

Figure 4. Expression of BSP-GFPtpz transgene expression during mineralization in vitro. (**A**) Representative images of a dental pulp culture from BSP-GFPtpz mice at different time points analyzed under phase contrast (BF) and epifluorescent lights for detection of BSP-GFPtpz and xylenol orange (XO). Primary cultures from dental pulp were prepared from 5- to 7-d-old hemizygous BSP-GFPtpz (Vijaykumar et al. 2019). Cultures were first grown in Dulbecco's Modified Eagle Medium, containing 10% fetal bovine serum. At day 7, mineralization was induced by addition of Minimum Essential Medium Alpha, 10% fetal bovine serum, with 50 μg/mL of fresh ascorbic acid and 4mM β-glycerophosphate. Medium was changed every other day. Note the expression of BSP-GFPtpz at days 10 to 21. (q–s) Higher magnification of culture at day 21 shows the expression of BSP-GFPtpz in XO-stained mineralized nodules (dotted lines). Scale bar: 2,000 μm. (**B**) Representative images of the same area of a primary dental pulp culture at D14 derived from BSP-GFPtpz/DSPP-Cerulean/DMP1-Cherry mice. The same area of culture was analyzed under bright (a) and epifluorescent lights for the detection of DMP1-Cherry (b), DSPP-Cerulean (c), and BSP-GFPtpz (d). The overlays (e–g) show the subpopulation of cells coexpressing DMP1-Cherry and DSPP-Cerulean (arrows in panel e) and cells coexpressing DMP1-Cherry and BSP-GFPtpz (arrows in panel f). Also, note lack of overlap between cells expressing BSP-GFPtpz and DSPP-Cerulean (g). Scale bar in all images: 200 μm.

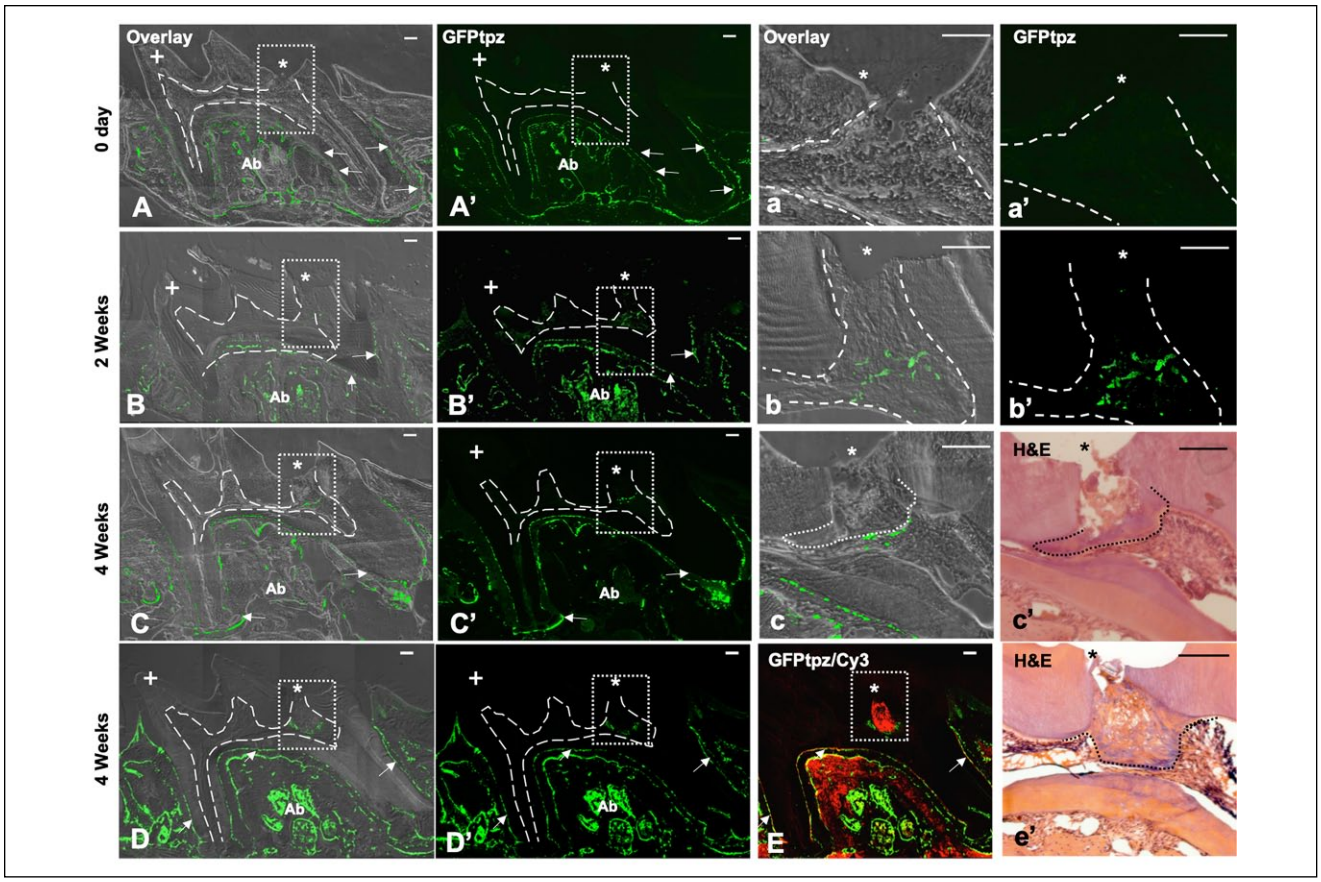

Figure 5. BSP-GFPtpz expression during reparative dentinogenesis. Representative epifluorescent images of sagittal sections of maxillary first molars with pulp exposure at day 0 (**A**, **A**′), 2 wk (**B**, **B**′), and 4 wk (**C**, **C**′, **D**, **E**) after pulp exposure. In all images, the dental pulp is denoted by dashed lines, the site of pulp exposure by an asterisk, and the control side without pulp exposure by a plus sign. Note the expression of BSP-GFPtpz by cementoblasts (arrows) and osteoblasts and osteocytes in alveolar bones (Ab). Also note the lack of expression of BSP-GFPtpz in the odontoblast layer lining the intact pulp in all images. (a, a′) Higher magnification of boxed area in panel A shows the site of exposure and the lack of BSP-GFPtpz^{+} in odontoblast layer and in pulp cells at the exposure site at day 0. (b, b′) Higher magnification of boxed area in panel B shows the appearance of BSP-GFPtpz in pulp cells below the site of exposure at 2 wk. (c) Higher magnification of boxed area in panel C shows BSP-GFPtpz^{+} cells lining the reparative dentin after 4 wk. (c′) A representative H&E-stained image of an adjacent section shows the reparative dentin at the site of pulp exposure. (c, c′) Reparative dentin is denoted by dotted lines. (D, e′) Images at 4 wk after pulp exposure stained with anti-BSP antibody shown in panel E. (E) A representative image at 4 wk after pulp exposure stained with anti-BSP antibody. Sections were permeabilized and stained with rabbit anti-BSP primary antibody, followed by donkey anti-rabbit Cy3 secondary antibody (1:200; Jackson ImmunoResearch) for 1 h at room temperature. Note that the reparative dentin tissue, alveolar bone, and cementum (arrows) but not dentin stain positive for anti-BSP antibody. (e′) A representative H&E-stained image of an adjacent section shows the reparative dentin at the site of pulp exposure. Reparative dentin is denoted by dotted lines. Scale bars in all images: 100 µm. H&E, hematoxylin and eosin.

was a small population (approximately 1% to 3%) of cells coexpressing BSP-GFPtpz^{+} and DMP1-Cherry^{+} cells in these cultures at days 10 and 14 (Fig. 4B; Appendix Fig. 3A–C).

Expression of BSP-GFPtpz Transgene in Reparative Dentinogenesis In Vivo

Several studies have shown BSP and *Bsp* expression in tertiary dentin (James et al. 2004; Yang et al. 2010; Vidovic et al. 2017). We next examined the expression of BSP-GFPtpz during reparative dentinogenesis using experimental pulp exposures established in our laboratory (Vidovic et al. 2017; Vidovic-Zdrilic et al. 2018). In these studies, experimental pulp exposure leading to adequate removal of dentin and destruction of odontoblasts (Vidovic et al. 2017; Vidovic-Zdrilic et al. 2018), which are essential for the initiation of reparative dentinogenesis, was created in 4-wk-old BSP-GFPtpz animals (Vidovic et al. 2017; Vidovic-Zdrilic et al. 2018).

Examination of teeth at 2 wk after pulp exposure showed the appearance of BSP-GFPtpz^{+} cells in dental pulp in close vicinity to the site of pulp exposure (Fig. 5B–b′). After 4 wk, BSP-GFPtpz^{+} cells were lining the reparative dentin that formed underneath the exposure site (Fig. 5C–c′). Immunocytochemical analysis of a section after 4 wk showed expression of BSP in the reparative dentin (Fig. 5D–e′).

Discussion

In the present study, we examined the expression of BSP-GFPtpz transgene in the teeth and bones and during reparative

dentinogenesis. The result showed that BSP-GFPtpz, *Bsp*, and BSP were not expressed in odontoblasts and dentin throughout various stages of tooth development. Following root formation, BSP-GFPtpz was expressed at high levels in cementoblasts. The lack of BSP-GFPtpz, *Bsp*, and BSP expression in odontoblasts during tooth development is consistent with observations in $Bsp^{-/-}$ mice. Despite substantial mineralization defects in the alveolar bone and cementum, $Bsp^{-/-}$ mice showed no abnormalities in odontoblasts, odontoblast markers, or physiologic dentinogenesis (Foster et al. 2015).

In bones, BSP-GFPtpz transgene was highly expressed by osteoblasts and some (but not all) osteocytes. Comparison of BSP-GFPtpz and DMP1-Cherry expression in long bones showed that BSP-GFPtpz was highly expressed in less mature osteoblasts whereas DMP1-Cherry was highly expressed in more mature osteoblasts and osteocytes.

Despite its lack of expression in dental pulp, odontoblasts, and physiologic dentin, BSP-GFPtpz$^+$ cells appeared and expanded during in vitro mineralization of pulp cultures and during reparative dentinogenesis. The exclusive and nonoverlapping expression of BSP-GFPtpz$^+$ and DSPP-Cerulean$^+$ in cultured cells indicated that, similar to endogenous BSP, BSP-GFPtpz$^+$ is activated and expressed by cells in the osteogenic lineages but not in the cells of the dentinogenic lineage.

BSP is expressed in tertiary dentin (Moses et al. 2006; Goldberg et al. 2008; Smith et al. 2012; Sangwan et al. 2013; Vidovic et al. 2017; da Rosa et al. 2018; Vidovic-Zdrilic et al. 2018) and can induce tertiary dentinogenesis (Decup et al. 2000; Six et al. 2002). Our study also showed the activation and expression of BSP-GFPtpz during reparative dentinogenesis. BSP-GFPtpz$^+$ cells were detected underneath the BSP$^+$ reparative dentin.

The expression of BSP-GFPtpz transgene during in vitro mineralization of dental pulp and during reparative dentinogenesis, which is consistent with the expression of BSP and *Bsp* reported by others, suggests that trauma and/or inflammation in dental pulp results in activation of the osteogenic program in resident progenitors in dental pulp. Reimplantation of the tooth and molar crowns resulted in formation of calcified tissue in pulp cavity composed of dentin-like tissue expressing Dspp and bone-like tissues expressing high levels of osteopontin and BSP (Takamori et al. 2008; Zhao et al. 2007). Pulp cultures derived from pulp 48 h after exposure showed enhanced osteogenic potential (Wang et al. 2013).

Although the underlying mechanisms of activation of the osteogenic program in dental pulp progenitors are not fully understood, the available evidence suggests possible involvement of Runx2, a master regulator of skeletal development. RUNX2 regulates the expression of members of the SIBLING family, including *Bsp, Dspp*, and *Dmp1*, through multiple *Runx2*-binding sites, and it is a target for several signaling pathways that regulate its phosphorylation, activation, and stabilization (Mevel et al. 2019).

Through the regulation of osterix (Sp7), Runx2 regulates the formation of preosteoblasts and immature osteoblasts, and Runx2 expression decreases with maturation of osteoblasts (Mevel et al. 2019). Transgenic mice that overexpressed Runx2 in osteoblasts with 2.3-kb Col1a1 promoter developed osteopenia caused by the inhibition of osteoblast maturation and accumulation of immature osteoblasts, indicating that Runx2 inhibits the late stage of osteoblast maturation while promoting early stages of osteoblast development (Kanatani et al. 2006; Li et al. 2011).

In teeth, *Runx2* is expressed in preodontoblasts but not in more differentiated odontoblasts (Camilleri and McDonald 2006). In vivo and in vitro studies have shown that overexpression of *Runx2* increased expression of DSPP in preodontoblasts but reduced its expression in mature odontoblasts (Chen et al. 2005; Miyazaki et al. 2008; Li et al. 2011). Transgenic mice overexpressing *Runx2* in odontoblasts at early and late stages of differentiation with 2.3-kb Col1a1 and *Dspp* promoter fragments displayed abnormalities in odontoblasts and dentin. In these animals, the sustained expression of Runx2 in odontoblasts inhibited terminal differentiation of odontoblasts and induced transdifferentiation of odontoblasts to bone-forming cells expressing osteocalcin and osteopontin (Miyazaki et al. 2008; Li et al. 2011). These findings suggest that Runx2 is involved in the cell fate determination (osteogenic vs. dentinogenic lineage) of pulpal mesenchymal progenitors. These observations suggest that growth factors and signaling molecules released during traumatic injury to dental pulp result in the sustained activation of Runx2, leading to activation of the osteogenic program in pulp progenitors.

Our previous observations showed that perivascular cells expressing alpha–smooth muscle actin (αSMA) constitute a population of mesenchymal progenitors in dental pulp capable of giving rise to *Dspp*$^+$ odontoblasts and *Bsp*$^+$ osteoblasts in reparative dentin (Vidovic et al. 2017). However, currently it is not known if αSMA$^+$ populations contain distinct osteogenic and dentinogenic populations or individual αSMA$^+$ cells that are multi- or bipotent.

By allowing the visualization of gene expression under various conditions, fluorescent protein reporter mice have provided valuable animal models for biological studies. One of the significant advantages of these animal models is that they provide investigators with the means to isolate and study intrinsically labeled cell populations. The temporal and spatial expression of BSP-GFPtpz transgene in the developing teeth, bone, and reparative dentin in vivo indicates that the 145-kb transgene contains many of the cis-regulatory elements necessary for regulating BSP gene expression in bone, cementum, and reparative dentin. The activation and expression of BSP-GFPtpz transgene in the osteogenic lineage in damaged dental pulp in vivo and in vitro provide an excellent experimental tool for further studies toward better understanding the differential activation of the osteogenic program in dental pulp and the effects of various growth factors and reagents on dentinogenic versus osteogenic differentiation of dental pulp stem/progenitors cells.

Author Contributions

A. Vijaykumar, M. Mina, contributed to conception, design, data acquisition, analysis, and interpretation, drafted and critically

revised the manuscript; P. Dyrkacz, I. Vidovic-Zdrilic, contributed to conception, design, data acquisition, and analysis, drafted the manuscript; P. Maye, contributed to conception, design, data acquisition, analysis, and interpretation, critically revised the manuscript. All authors gave final approval and agree to be accountable for all aspects of the work.

Acknowledgments

We thank all the individuals who provided reagents, valuable input, and technical assistance in various aspects of this study, including Barbara Rodgers, Dr. Evan Jellison, and UConn Health Flow Cytometry Core. This work was supported by grants from the National Institutes of Health / National Institute of Dental and Craniofacial Research (R01-DE016689 and T90-DE022526). The authors declare no potential conflicts of interest with respect to the authorship and/or publication of this article.

ORCID iD

A. Vijaykumar https://orcid.org/0000-0002-9311-8715

References

Balic A, Mina M. 2005. Analysis of developmental potentials of dental pulp in vitro using GFP transgenes. Orthod Craniofac Res. 8(4):252–258.

Balic A, Mina M. 2011. Identification of secretory odontoblasts using DMP1-GFP transgenic mice. Bone. 48(4):927–937.

Bellahcene A, Castronovo V, Ogbureke KU, Fisher LW, Fedarko NS. 2008. Small integrin-binding ligand N-linked glycoproteins (SIBLINGs): multifunctional proteins in cancer. Nat Rev Cancer. 8(3):212–226.

Bosshardt DD, Zalzal S, McKee MD, Nanci A. 1998. Developmental appearance and distribution of bone sialoprotein and osteopontin in human and rat cementum. Anat Rec. 250(1):13–33.

Bouleftour W, Juignet L, Bouet G, Granito RN, Vanden-Bossche A, Laroche N, Aubin JE, Lafage-Proust MH, Vico L, Malaval L. 2016. The role of the sibling, bone sialoprotein in skeletal biology—contribution of mouse experimental genetics. Matrix Biol. 52–54:60–77.

Butler WT, Ritchie H. 1995. The nature and functional significance of dentin extracellular matrix proteins. Int J Dev Biol. 39(1):169–179.

Camilleri S, McDonald F. 2006. Runx2 and dental development. Eur J Oral Sci. 114(5):361–373.

Chen S, Chen L, Jahangiri A, Chen B, Wu Y, Chuang HH, Qin C, MacDougall M. 2008. Expression and processing of small integrin-binding ligand n-linked glycoproteins in mouse odontoblastic cells. Arch Oral Biol. 53(9):879–889.

Chen S, Rani S, Wu Y, Unterbrink A, Gu TT, Gluhak-Heinrich J, Chuang HH, Macdougall M. 2005. Differential regulation of dentin sialophosphoprotein expression by Runx2 during odontoblast cytodifferentiation. J Biol Chem. 280(33):29717–29727.

da Rosa WLO, Piva E, da Silva AF. 2018. Disclosing the physiology of pulp tissue for vital pulp therapy. Int Endod J. 51(8):829–846.

Decup F, Six N, Palmier B, Buch D, Lasfargues JJ, Salih E, Goldberg M. 2000. Bone sialoprotein-induced reparative dentinogenesis in the pulp of rat's molar. Clin Oral Investig. 4(2):110–119.

Dyment NA, Jiang X, Chen L, Hong SH, Adams DJ, Ackert-Bicknell C, Shin DG, Rowe DW. 2016. High-throughput, multi-image cryohistology of mineralized tissues. J Vis Exp. 115. doi:10.3791/54468.

Fisher LW, Fedarko NS. 2003. Six genes expressed in bones and teeth encode the current members of the sibling family of proteins. Connect Tissue Res. 44 Suppl 1:33–40.

Foster BL, Ao M, Willoughby C, Soenjaya Y, Holm E, Lukashova L, Tran AB, Wimer HF, Zerfas PM, Nociti FH Jr, et al. 2015. Mineralization defects in cementum and craniofacial bone from loss of bone sialoprotein. Bone. 78:150–164.

Foster BL, Soenjaya Y, Nociti FH Jr, Holm E, Zerfas PM, Wimer HF, Holdsworth DW, Aubin JE, Hunter GK, Goldberg HA, et al. 2013. Deficiency in acellular cementum and periodontal attachment in Bsp null mice. J Dent Res. 92(2):166–172.

Fu Y, Maye P. 2015. Derivation of chondrocyte and osteoblast reporter mouse embryonic stem cell lines. Genesis. 53(3–4):294–298.

Fujisawa R, Butler WT, Brunn JC, Zhou HY, Kuboki Y. 1993. Differences in composition of cell-attachment sialoproteins between dentin and bone. J Dent Res. 72(8):1222–1226.

Ganss B, Kim RH, Sodek J. 1999. Bone sialoprotein. Crit Rev Oral Biol Med. 10(1):79–98.

Goldberg M, Lacerda-Pinheiro S, Priam F, Jegat N, Six N, Bonnefoix M, Septier D, Chaussain-Miller C, Veis A, Denbesten P, et al. 2008. Matricellular molecules and odontoblast progenitors as tools for dentin repair and regeneration. Clin Oral Investig. 12(2):109–112.

James MJ, Jarvinen E, Thesleff I. 2004. Bono1: a gene associated with regions of deposition of bone and dentine. Gene Expr Patterns. 4(5):595–599.

Kanatani N, Fujita T, Fukuyama R, Liu W, Yoshida CA, Moriishi T, Yamana K, Miyazaki T, Toyosawa S, Komori T. 2006. Cbf beta regulates Runx2 function isoform-dependently in postnatal bone development. Dev Biol. 296(1):48–61.

Li S, Kong H, Yao N, Yu Q, Wang P, Lin Y, Wang J, Kuang R, Zhao X, Xu J, et al. 2011. The role of runt-related transcription factor 2 (Runx2) in the late stage of odontoblast differentiation and dentin formation. Biochem Biophys Res Commun. 410(3):698–704.

Maye P, Stover ML, Liu Y, Rowe DW, Gong S, Lichtler AC. 2009. A BAC-bacterial recombination method to generate physically linked multiple gene reporter DNA constructs. BMC Biotechnol. 9:20.

Mevel R, Draper JE, Lie-A-Ling M, Kouskoff V, Lacaud G. 2019. Runx transcription factors: orchestrators of development. Development. 146(17):dev148296.

Miyazaki T, Kanatani N, Rokutanda S, Yoshida C, Toyosawa S, Nakamura R, Takada S, Komori T. 2008. Inhibition of the terminal differentiation of odontoblasts and their transdifferentiation into osteoblasts in Runx2 transgenic mice. Arch Histol Cytol. 71(2):131–146.

Moses KD, Butler WT, Qin C. 2006. Immunohistochemical study of small integrin-binding ligand, N-linked glycoproteins in reactionary dentin of rat molars at different ages. Eur J Oral Sci. 114(3):216–222.

Qin C, Brunn JC, Jones J, George A, Ramachandran A, Gorski JP, Butler WT. 2001. A comparative study of sialic acid–rich proteins in rat bone and dentin. Eur J Oral Sci. 109(2):133–141.

Qin C, D'Souza R, Feng JQ. 2007. Dentin matrix protein 1 (DMP1): new and important roles for biomineralization and phosphate homeostasis. J Dent Res. 86(12):1134–1141.

Sangwan P, Sangwan A, Duhan J, Rohilla A. 2013. Tertiary dentinogenesis with calcium hydroxide: a review of proposed mechanisms. Int Endod J. 46(1):3–19.

Six N, Decup F, Lasfargues JJ, Salih E, Goldberg M. 2002. Osteogenic proteins (bone sialoprotein and bone morphogenetic protein-7) and dental pulp mineralization. J Mater Sci Mater Med. 13(2):225–232.

Smith AJ, Scheven BA, Takahashi Y, Ferracane JL, Shelton RM, Cooper PR. 2012. Dentine as a bioactive extracellular matrix. Arch Oral Biol. 57(2):109–121.

Staines KA, MacRae VE, Farquharson C. 2012. The importance of the sibling family of proteins on skeletal mineralisation and bone remodelling. J Endocrinol. 214(3):241–255.

Strecker S, Fu Y, Liu Y, Maye P. 2013. Generation and characterization of osterix-cherry reporter mice. Genesis. 51(4):246–258.

Takamori Y, Suzuki H, Nakakura-Ohshima K, Cai J, Cho SW, Jung HS, Ohshima H. 2008. Capacity of dental pulp differentiation in mouse molars as demonstrated by allogenic tooth transplantation. J Histochem Cytochem. 56(12):1075–1086.

Vidovic I, Banerjee A, Fatahi R, Matthews BG, Dyment NA, Kalajzic I, Mina M. 2017. Alphasma-expressing perivascular cells represent dental pulp progenitors in vivo. J Dent Res. 96(3):323–330.

Vidovic-Zdrilic I, Vining KH, Vijaykumar A, Kalajzic I, Mooney DJ, Mina M. 2018. FGF2 enhances odontoblast differentiation by αSMA^{+} progenitors in vivo. J Dent Res. 97(10):1170–1177.

Vijaykumar A, Ghassem-Zadeh S, Vidovic-Zdrilic I, Komitas K, Adameyko I, Krivanek J, Fu Y, Maye P, Mina M. 2019. Generation and characterization of DSPP-cerulean/DMP1-Cherry reporter mice. Genesis. 57(10):e23324.

Wang Y, Yan M, Wang Z, Wu J, Wang Z, Zheng Y, Yu J. 2013. Dental pulp stem cells from traumatically exposed pulps exhibited an enhanced osteogenic potential and weakened odontogenic capacity. Arch Oral Biol. 58(11):1709–1717.

Yang IS, Lee DS, Park JT, Kim HJ, Son HH, Park JC. 2010. Tertiary dentin formation after direct pulp capping with odontogenic ameloblast-associated protein in rat teeth. J Endod. 36(12):1956–1962.

Zhao C, Hosoya A, Kurita H, Hu T, Hiraga T, Ninomiya T, Yoshiba K, Yoshiba N, Takahashi M, Kurashina K, et al. 2007. Immunohistochemical study of hard tissue formation in the rat pulp cavity after tooth replantation. Arch Oral Biol. 52(10):945–953.